Effectiveness of a Ventilated Concrete Slab on an Air Source Heat Pump Performance in Cold Climate

Navid Ekrami[1], Raghad S. Kamel[1], and Alan S. Fung[1]

[1]Department of Mechanical and Industrial Engineering, Ryerson University, 350 Victoria Street, Toronto, Ontario, Canada M5B 2K3

Abstract

This article studies the effect of a ventilated concrete slab (VCS) as thermal storage in buildings. The VCS is coupled with a combined building integrated photovoltaic/thermal (BIPV/T) collector and air source heat pump (ASHP). Design criteria of the air channels inside the slab are discussed considering the mass flow rate of air and size of channels. A TRNSYS model of BIPV/T systems was used to estimate potential thermal generation of the panels in the winter. Generated thermal energy was stored in the VCS and released to the ASHP inlet during night. It is shown that using VCS thermal storage to preheat the outdoor air as an inlet flow to the air source heat pump increases the coefficient of performance (COP) of the system. Consequently, power consumption decreases during night. This thermal storage improves performance of both PV/T and ASHP without utilizing water or other thermal storage systems/materials.

1 Introduction

Residential energy consumption in cold climate areas is primarily for space and domestic hot water (DHW) heating. In Canada, about 17% of the annual national end use energy is for to the residential sector (Statistics Canada, 2009); this amount corresponds to 233 kWh per square meter of floor area in 2006 (Natural Resources Canada, 2009). In addition, 59% of the residential energy consumption is for space heating and 18% for DHW heating (Natural Resources Canada, 2009). Significant energy and cost savings could be achievable by integrating sustainable and state of the art renewable technologies in one combined system (Athienitis, 1997). This study focuses on the design and integration of a Thermal Energy Storage (TES) and BIPV/T system into an Air Source Heat Pump (ASHP) in a residential house in Canada. The general approach in the design of this integrated system is to consider a house in a cold, but relatively sunny climate.

In cold climatic weather, during winter, the thermal energy could be collected by solar collectors. Generated thermal energy may not be warm enough to be useful for direct heating but it may be used as a source for the heat pump (Athienitis et al., 2000; Gang et al, 2007). Since the solar collection system can supply energy at temperatures higher than the ambient outdoor air, the overall performance and coefficient off performance (COP) of the heat pump would increase over that for the heat pump. Also, combined heating system would seem to operate more economically (Badescu, 2002). The disadvantage of solar based system appears for the discrepancy between the supply and the demand. Considering that the heat demand is at

maximum in winter, or at night, when the supply of solar energy is minimal or zero. This makes the thermal storage an essential part of a solar powered heat pump system. The operation of a TES unit is similar to a common heat exchanger. However, the TES unit is either being charged or discharged at a given time, so that its operation is essentially unsteady (Badescu, 2003).

Those thermal energy storage (TES) systems that are parts of building such as wall and slab are defined as Building Integrated Thermal Energy Storage (BITES) Systems (Chen et al., 2013B). BITES systems with proper control strategies will improve the thermal performance of buildings by reducing room temperature fluctuations, decreasing total space cooling/ heating energy consumption. BITES systems also shift and shave peak energy demands, and reduce the discrepancy of energy supply/availability and demand (Dincer, 2002). Active BITES systems include hydronic, ventilated, electric, and capillary systems. Hydronic systems are often designated as thermo-active building systems (TABS) when significant thermal storage is integrated (generally thicker than 5 cm of concrete) such as ventilated concrete slabs.

Although active BITES systems offer more features compare to passive ones, an accurate model is needed to assess and compare the thermal response characteristics of different alternatives. Detailed models require more detailed knowledge of geometry, which may not be known in the early design stages. Simplified models are also needed for whole building simulations over long simulation periods. The weather forecast information and corresponding space heating/cooling load predicted from building models are needed as inputs for the control of BITES systems (Chen et al., 2013A)

2 Methodology

In order to investigate the effect of a Ventilated Concrete Slab (VCS) as a thermal storage on the overall performance of the BIPV/T + ASHP system, a test hut is designed and planned to be built at Toronto and Region Conservation Authority (TRCA). The test hut would be equipped with an ASHP, which is integrated with PV/T panels to improve the performance of the system. Moreover, the floor of the test hut is designed to be used as a Thermal Energy Storage (TES) as it is shown in Figure 1 and 2. Stored thermal energy during sunny hours can be used to increase the inlet air temperature for the ASHP during night time. This configuration is expected to enhance the overall performance of the integrated system by implementing the TES.

Besides the structural function of VCS as a floor slab, the VCS also can serve as actively charged thermal mass to store solar thermal energy and then passively release it to assist space heating (Ren *et al.*, 1998; Zmeureanu *et al.*, 1988). The VCS is designed to be charged with solar-heated outdoor air in an open loop configuration. It is based on commonly available construction technologies and can thus be easily implemented in North American homes. Garage slab as an unconditioned space or floor slab as conditioned slab are different options that can be considered for houses. A steel deck can be easily placed under the floor concrete during the construction and spaces between the edges can be used as air channels through the slab.

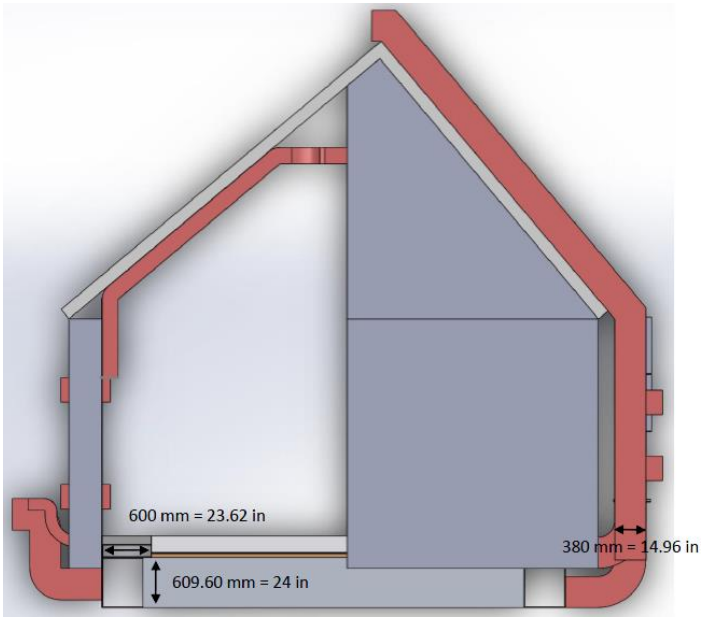

Figure 1 - Cross Section View of the Test Hut

2.1 Design criteria of ventilated concrete slab

In order to design an efficient VCS, The number of air channels and their total cross sectional area need to suit the air flow rate of the BIPV/T system. It is important to distribute air flow through all channels evenly to maximize the Convective Heat Transfer Coefficient (CHTC) and minimize the friction loss (Krauter *et al.*, 1999). Also, the floor must not be overheated. The comfortable temperature range for concrete slab surface (with no cover) is between 26 and 28.5 ^{o}C for people with bare feet (ASHRAE, 2005); and 19–29 ^{o}C for people wearing lightweight indoor shoes in office environment (ASHRAE, 2004). Therefore, thickness of the concrete slab is critical not only for storage capability but also for human thermal comfort. Suitable amount of concrete is needed to absorb maximum heat without surface overheating or releasing heat passively in an appropriate rate. Too much concrete increases cost and structural load. Bottom heat loss to soil underneath must be minimized through use of suitable insulation.

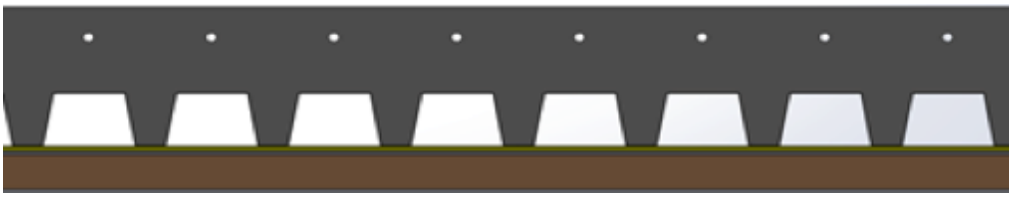

Figure 2 - Cross Section Schematic of the Floor

Design of the VCS is interrelated with the design of the house and the BIPV/T system. The sizing of the steel deck and the concrete slab are related to the thermal capacitance and the heating load of the house, the thermal energy output of the BIPT/T roof, the geometry of the basement, the CHTC inside the VCS channels, the prevention of top surface overheating of the VCS, and the structural design considerations.

3 Preliminary Analysis

The very first criterion that needs to be decided is the size of the metal deck and the concrete thickness. Air velocity in the channels and the hydraulic diameter are determined by the

cross section area. The Reynolds number is related to the air velocity, mass flow rate, and hydraulic diameter. The CHTC is based on Reynolds number. Moreover, the channel perimeter and the CHTC determine convective conductance inside the air channel. Therefore, both the geometry and size of the cross section of the air channel are the key design parameters.

If the lengths of the channels are long enough, the slab can recover the maximum heat possible from the heated air, and the temperature of the outlet air will be almost the same as the temperature of the concrete near the outlet. However, longer air channel will result in higher friction loss. The thickness of the slab affects the amount of thermal energy that can be stored, and the rate of storage/release. According to the PV/T design properties, the air mass flow rate is estimated. Therefore, required CHTC for maximum heat recovery,$U_{c-required}$, can be calculated from following equation (Chen *et al.*, 2013B).

$$U_{c-required} = \frac{\dot{m} \times C_{p.air} \times \Delta T_b}{No_{ch} \times L_{ch} \times \Delta T_{LMTD}} \quad (1)$$

$$\Delta T_{LMTD} = \frac{\Delta T_{out} - \Delta T_{in}}{\ln(\frac{\Delta T_{out}}{\Delta T_{in}})} \quad (2)$$

If the maximum heat from the air is recovered by the slab, the outlet air temperature will be very close to the slab temperature.

CHTC, U_c, and $U_{c-required}$ were estimated using the following equations (Stephenson, 1971) for different cross sections of air channels based on various steel deck types available in the market.

$$U_c = (2 \times H_{channel} \times W_{channel}) \times h_c \quad (3)$$

Where $h_c = Nu \times \frac{k_{air}}{D_h}$ (4)

$$Nu = \frac{f}{8} \times Re \times Pr_{air}^{\frac{1}{3}} \quad (5)$$

$$Re = \frac{\rho_{air} \times v_{air} \times D_h}{\mu_{air}} \quad (6)$$

In order to calculate Darcy friction factor (f) following equation was used; (data from Moody Chart)

$$\frac{1}{\sqrt{f}} = -2 \times \log(\frac{\varepsilon/D_h}{3.7} + \frac{2.51}{Re \times \sqrt{f}}) \quad \text{(Eq. 7)}$$

Using friction factor of 0.08 the U_c equation can be simplified to (Chen *et al.*, 2013A):

$$U_c = C \times FlowRate_{channel}(\frac{2}{W_{channel}} + \frac{1}{H_{channel}}) \quad \text{(Eq. 8)}$$

Where $C = \frac{\rho_{air} \times k_{air} \times Pr^{\frac{1}{3}}}{100 \mu_{air}}$ and $FlowRate_{channel}$ is flow rate inside each channel.

Accordingly, U_c was calculated based on various flow rates and different channel configurations. Since the test hut floor area is 9 meter by 6 meter, there are two options for channels set up. They can either placed along the 9 meter length of the floor or along the 6 meter width of the floor. The center to center standard distance between channels for the steel deck is 152

mm, therefore, 60 channels can be set up along the 9 m side of the floor (each 6 meter long) or 40 channels can be placed along the 6 meter side of the floor with the length of 9 meter.

Figure 3 shows how convective conductance varies with different flow rates. Figure 3 also shows how U_c changes with different number of channels and two standard height of channels. Interestingly, the channel configuration with the number of 40 and height of 38 mm would have the highest convective conductance per meter and 60 channel with 76 mm height setting would have the lowest U_c.

Moreover, convective conductance for each meter of channels was carried out based on different height of the channel when the width of channel was constant at 114 mm. Results are shown in Figure 4. U_c for all of the configurations decrease when the channel height increases.

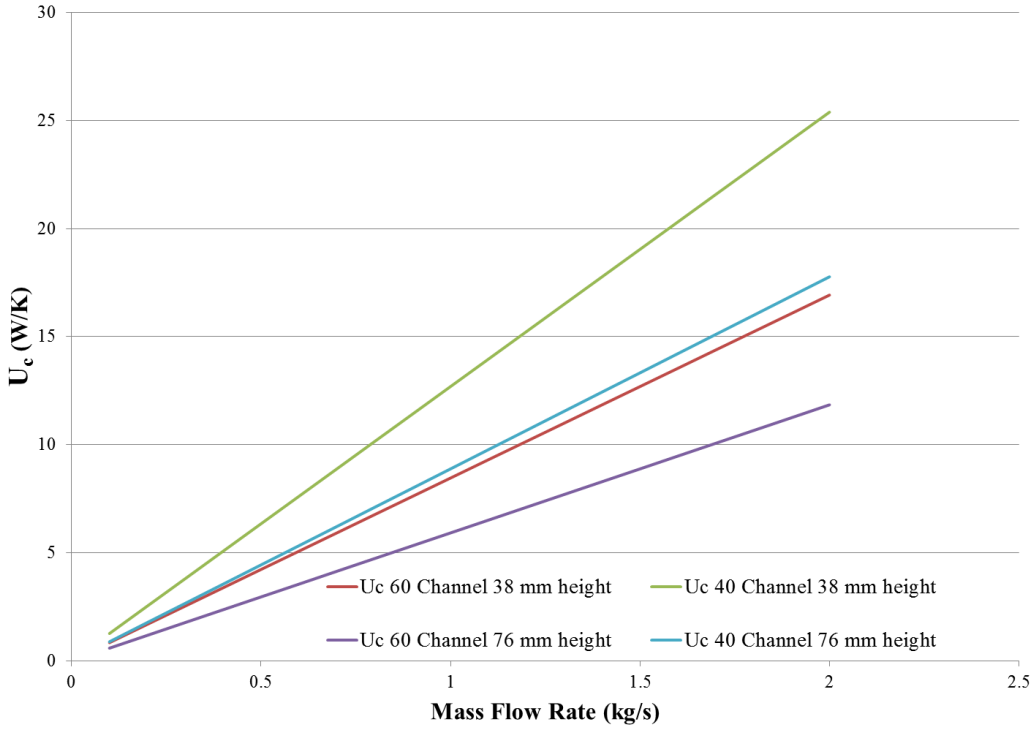

Figure 3 - Convective Conductance inside channels vs mass flow rate

Required U_c varies with different temperature settings. Three different scenarios for the temperature settings were defined, which is shown in Table 1 as follows:

Table 1: Temperature Settings of Air & Concrete

	Setting A	Setting B	Setting C
Air Temperature Leaving the Slab (°C)	2	17	19
Air Temperature Entering the Slab (°C)	12	25	28
Concrete Outlet Temperature (°C)	1	15	16
Concrete Inlet Temperature (°C)	-10	5	5

The slope of $U_{c\text{-require}}$ line varies with different temperature settings. When the $U_{c\text{-require}}$ is lower, it is more possible to meet the condition. Figure 4 also shows various $U_{c\text{-require}}$ of three different temperature settings with different mass flow rates versus U_c of different channel configurations and air channel heights.

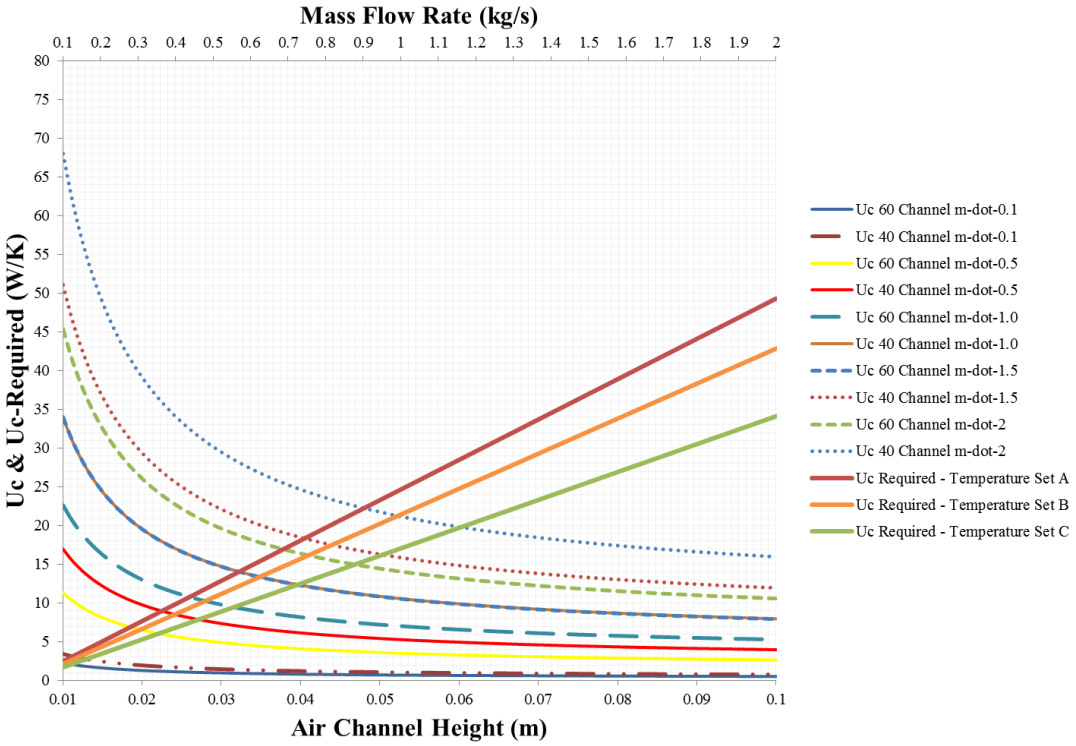

Figure 4 - U & Uc-require for different mass flow rates and air channel heights

4 Energy Storage Calculation

Energy calculations were performed in order to study the potentials of the concrete slab as a thermal storage. Again three different temperature setting were defined (Table 1). Based on those temperature set points for air and concrete Figure 5 was developed. Figure 5 illustrates that the concrete slab potentially is capable to store with different rates depending on the mass flow rate. The rate of energy storage could be up to 20 kW.

Although the rate of energy storage in the VCS is high, the BIPV/T cannot provide required thermal energy for the storage due to radiation limits in winter days based on Toronto weather conditions. Since sunny hours are less and radiation level is lower in winter compare to summer, the thermal energy generated by the BIPV/T system is lower than the VCS capacity.

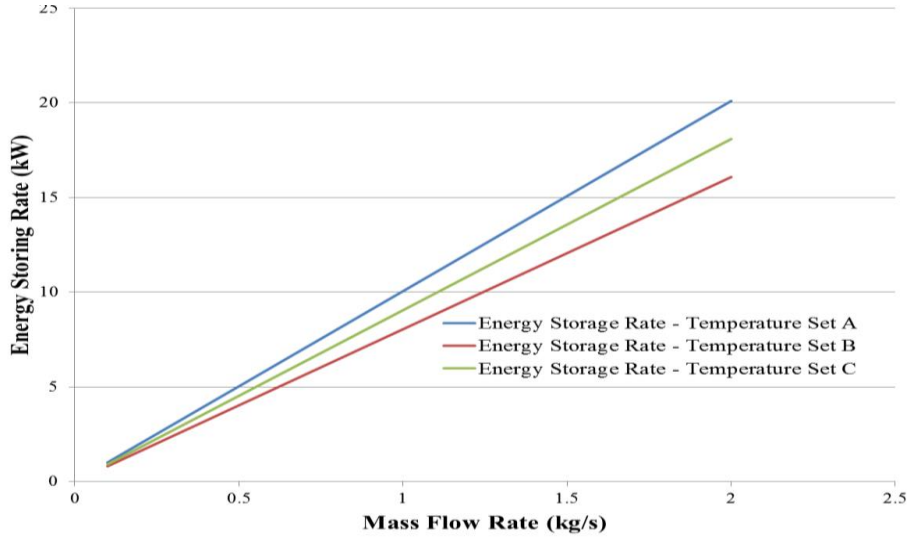

Figure 5 - Energy Storage Rate vs Mass Flow Rate

Figure 6 shows the thermal energy generation of a 5x5 PV/T panels. Figure 6 is generated based on results of the simulation model of the test hut in TRNSYS (Kamel *et al.*, 2013). The graph shows the thermal energy generation in a typical winter day of Toronto (January 21st). Two different mass flow rates are considered and the higher flow rate results in higher energy generation. The average thermal energy generation is 7.6 kW for 2 kg/s mass flow rate and 5.1 kW for 0.5 kg/s flow rate. The outlet temperature also varies according to the radiation level.

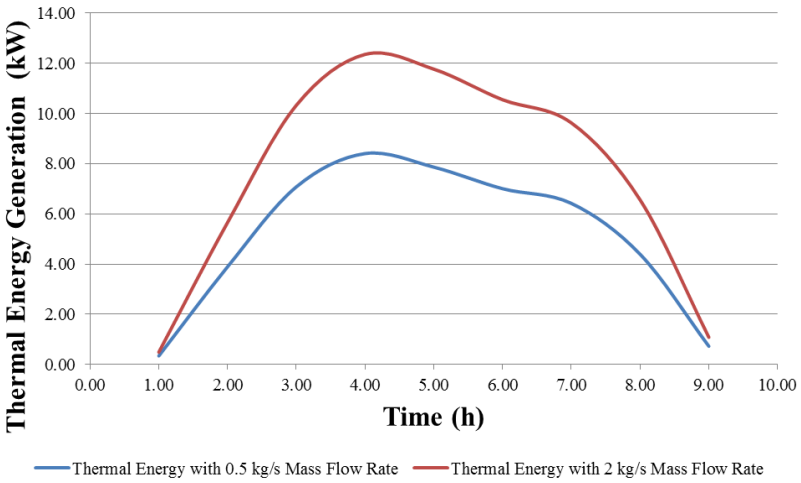

Figure 6 - Thermal Energy Generation by PV/T panels during a Typical Winter Day

Additionally, concrete thickness with respect to temperature change in concrete was studied. As Figure 7 shows, assuming a constant amount of energy to be stored in the slab, the temperature change varies. Figure 7 also shows that the channels with 38 mm height will have higher delta T compared to those channels with 76 mm height. Note that Figure 7 is generated based on 50 kWh energy storage, considering that the heat capacity and the density of the concrete are 0.96 kJ/kg.K and 2400 kg/m^3 respectively.

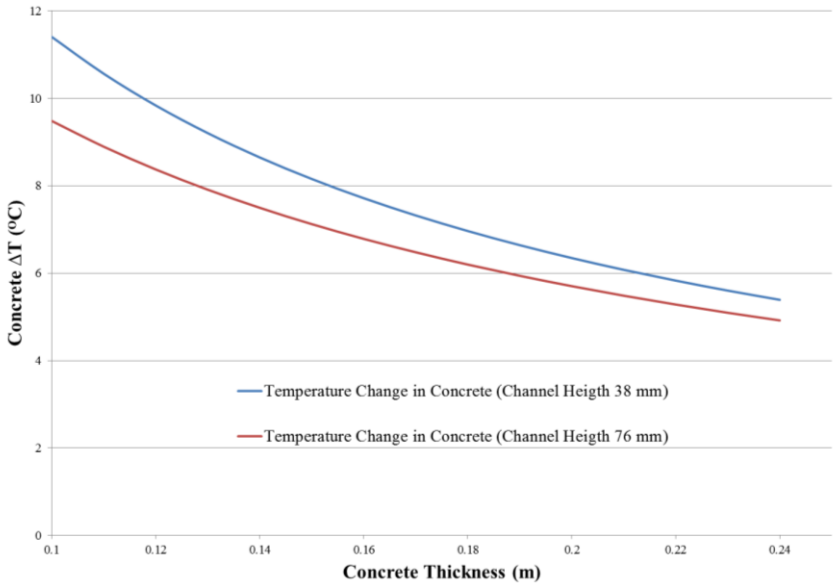

Figure 7 - Temperature Change in the Slab vs Thickness

In order to design an integrated system many influencing variables are required to be known. According to literature, this type of VCS can increase the ambient temperature by 7 ^{O}C

which depends on many variables. Although the slab increases the outdoor temperature when the air passes through the channels, after few hours, when the slab is discharged, the outlet temperature converges to the ambient temperature. Figure 8 shows the outlet temperature of the slab during discharge period when the ambient temperature is -11 ^{O}C.

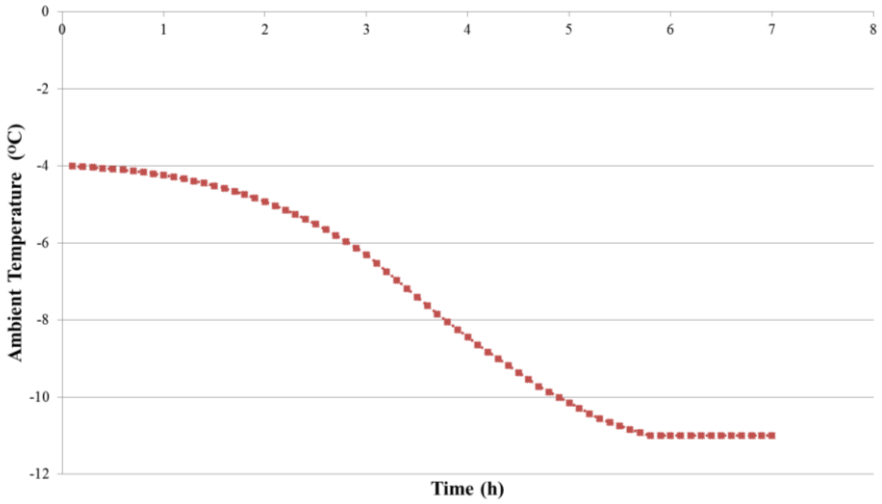

Figure 8 - Outlet Air Temperature during Discharge

It has been shown experimentally that the COP of ASHP has a linear relation with ambient temperature (Safa *et al.*, 2012; Safa, 2011). The higher outdoor temperature results in higher COP as shown in Figure 9.

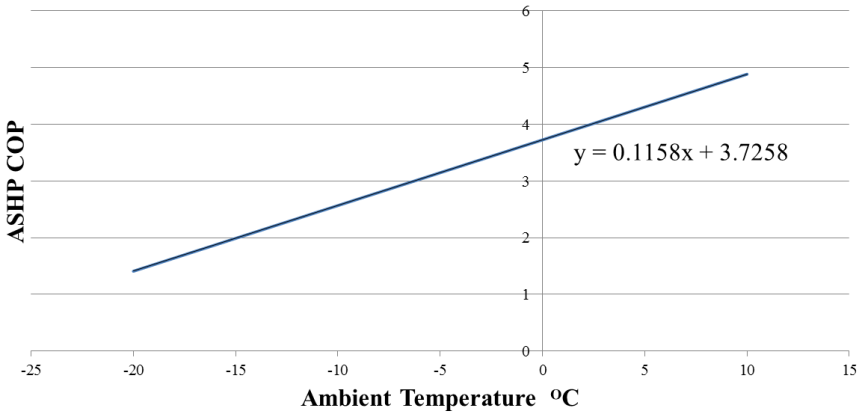

Figure 9 - The COP of ASHP vs Ambient Temperature

The Figure compares the COP of an ASHP at -11^{O}C with and without thermal storage. It is shown that when a concrete slab as a thermal storage is integrated to an ASHP can enhance the overall performance of the system.

The power consumption and the overall performance of the air source heat pump were also studied. Figure 10 shows and compares the COP and power consumption of the ASHP with and without VCS. It is shown that, as expected, the power consumption of the ASHP decreases using a VCS. The results shows that when a concrete slab as a thermal storage is integrated to an ASHP can enhance the overall performance of the system. Interestingly, when the ambient temperature is very cold the VCS has positive effect in both COP and power consumption of the ASHP. If the ambient temperature is not too cold, although the VCS improves the overall performance, it is less effective. Therefore, the VCS is a potential perfect solution for very cold winter nights.

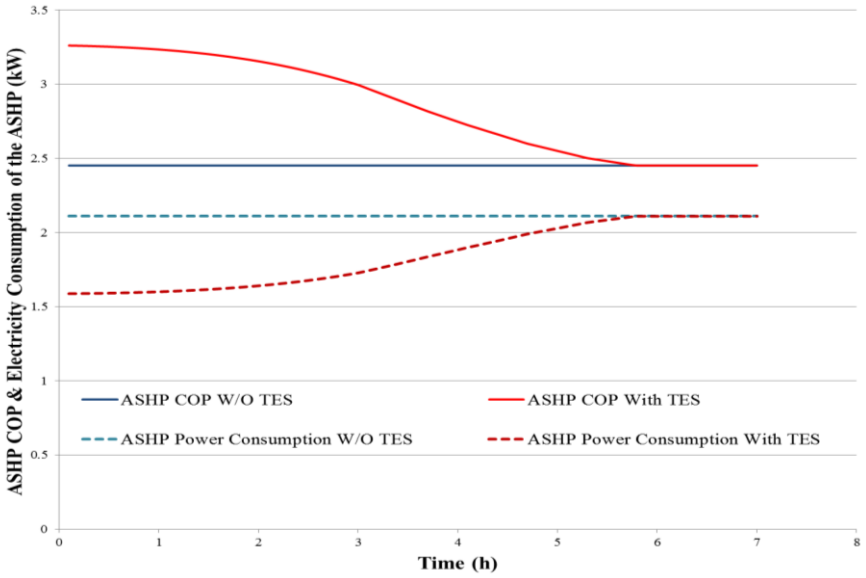

Figure 10 - COP and Power Consumption of an ASHP with and without TES

In order to investigate the effectiveness of the TES with respect to different cold ambient temperature, Figure 11 was produced. Figure 11 shows the difference between the electricity consumption of ASHP when it is integrated to a TES and without TES. As previously noted, higher electricity saving was achieved when the outdoor temperature was low. It is because the COP of ASHP without TES is lower when the outdoor air temperature is colder while heating demand is at its highest.

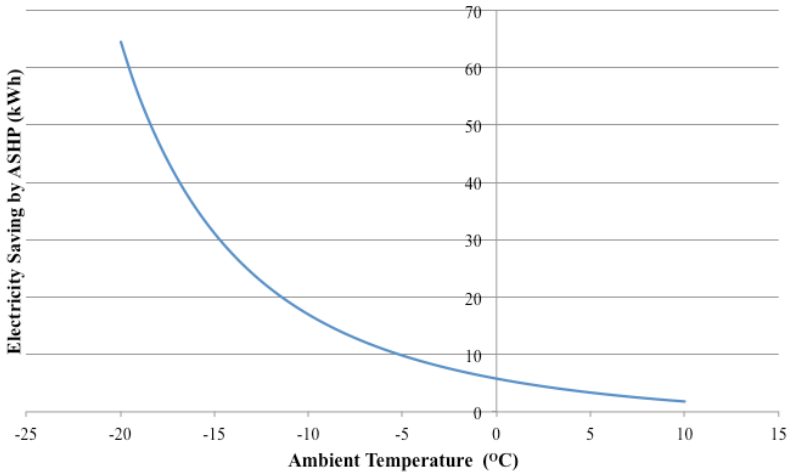

Figure 11 - Electricity Saving due to Using TES with respect to Outdoor Temperature

5 Remarks

Preliminary analysis shows that an integrated TES+BIPV/T+ASHP will increase the over-all COP of the system. Therefore, this system is expected to reduce the operational cost.

The study shows that heat transfer rate between air and slab varies due to many variables such as air velocity, width and height of air channel, number of channels, channel length, outdoor temperature, and slab initial temperature.

The performance of the system changes when the space above the slab is conditioned compared to an unconditioned space. Design criteria for the concrete slab as TES and also initial conditions in the calculations varies due to different temperature settings.

This article is a preliminary study for integrating a TES in combined BIPV/T and ASHP system. More detailed numerical and experimental work as well as optimization of design and operation of the system is required. Also a detailed simulated model is essential to be developed in order to study all aspects of the system. The proposed system will be experimentally tested in spring 2014 to verify the feasibility analysis and simulation results.

6 Nomenclature

D_h	Hydraulic diameter [m]	Pr	Prandtl number [-]
f	Darcy fricition factor [-]	Re	Reynolds number [-]
$H_{channel}$	Channel hight [m]	ρ_{air}	Air density [kg/m^3]
h_c	Convection heat transfer coefficient [W K^{-1}m^{-2}]	v_{air}	Air velocity [m/s]
k_{air}	Thermal conductivity of air flowing in the duct [W K^{-1}m^{-2}]	μ_{air}	Air dynamic viscosity [kg/m. s]
$\dot{m}$	Air mass flow rate [kg/s]	ε	Roughness [m]
Nu	Nusselt number [-]		
No_{ch}	Number of Channels		
Pr	Prandtl number [-]		
Re	Reynolds number [-]		
T_{in}	Inlet temperature [°C]		
T_{out}	Outlet temperature [°C]		
U_c	Convective Conductance inside air channel per meter lenghth of channel [W/K]		
$W_{channel}$	Channel Width [m]		
ΔT_{LMTD}	Log Mean Temperature Difference (LMTD) between the slab and the heated air [°C]		
ΔT_b	Bulk Temperature difference at inlet and outlet		

7 Acknowledgements

The authors would like to acknowledge the funding support for this project from the Natural Sciences and Engineering Research Council (NSERC) of Canada, Toronto Atmospheric Fund (TAF), MITACS, and Ontario Graduate Scholarship (OGS).

8 References

ASHRAE, 2004. Standard 55: Thermal Environmental Conditions for Human Occupancy. American Society of Heating Refrigerating and Air-Conditioning Engineers (ASHRAE), Atlanta, GA.

ASHRAE, 2005. ASHRAE Handbook, SI ed. In: Fundamentals American Society of Heating, Refrigerating, and Air-Conditioning Engineers (ASHRAE), Atlanta, GA.

Athienitis, A.K. , Chen, Y. (2000) "The effect of solar radiation on dynamic thermal performance of floor heating systems", *Solar Energy*, 69(3), 229-237

Athienitis, A.K. (1997) " Investigation of thermal performance of a passive solar building with floor radiant heating", *Solar Energy*, 61(5), 337-345

Badescu, V., "Model of a Solar-Assisted Heat-Pump System for Space Heating Integrating a Thermal Energy Storage Unit", *Energy and Building*, 2002: 715-726.

Badescu, V., "Model of a Thermal Energy Storage Device Integrated into a Solar-Assisted Heat-Pump System for Space Heating", *Energy Conversion and Management*, 2003:1589-1604.

Chen, Y., Athienitis, A.K., Galai, K., "Thermal performance and charge control strategy of a Ventilated Concrete Slab (VCS) with active cooling using outdoor air", *ASHRAE Transactions*, Vol. 118, Issue PART 2, 2012, pp. 556-568

Chen, Y., Athienitis, A. K., & Galal, K. E. (2013A). Frequency domain and finite difference modeling of ventilated concrete slabs and comparison with field measurements: Part 2. Application. *International Journal of Heat and Mass Transfer*

Chen, Y., Athienitis, A. K., & Galal, K. E. (2013B). Frequency domain and finite difference modeling of ventilated concrete slabs and comparison with field measurements: Part 1, modeling methodology. *International Journal of Heat and Mass Transfer*

Dincer, I. (2002) "On thermal energy storage systems and applications in buildings", *Energy and Buildings*, 34 (4), 377-388

Gang, P., Jie, J., Wei, H., Keliang, L., and Hanfeng, H., 2007, "Performance of Photovoltaic Solar Assisted Heat Pump System in Typical Climate Zone", *Energy and Environment.* Vol. 6.

Kamel, R. S., Fung, A. S. and Noire, Q.,"Feasibility of Building Integrated Photovoltaic-Thermal Collector (BIPV/T) with Two-stage Variable Capacity Air Source Heat Pump in Canada", *3rd climate change technology conference*,May 27-29, 2013, Concordia University, Montreal, Canada.

Krauter, S., Araújo, R.G., Schroer, S., Hanitsch, R., Salhi, M.J., Triebel, C., Lemoine, R. (1999) "Combined photovoltaic and solar thermal systems for facade integration and building insulation", *Solar Energy*,67(4-6), 239-248

Natural Resources Canada, 'Residential End-Use Model', (2009). Last visit: February 2014, http://www.oee.nrcan.gc.ca/corporate/statistics/neud/dpa/tablestrends2/res_ca_2_e_3.cfm?attr=0

Ren, M. J., & Wright, J. A. (1998). A ventilated slab thermal storage system model. *Building and Environment, 33*(1), 43-52.

Safa, A. A., Performance Analysis of A Two-stage Variable Capacity Air Source Heat Pump and A Horizontal Loop Coupled Ground Source Heat Pump System. MASc thesis, Mechanical and Industrial Engineering, Ryerson University, 2012.

Safa, Amir A., Fung, Alan S., and Leong, Wey H., "Part Load Performance of a Two-stage Variable Speed Air Source Heat Pump System in Cooling Mode", *ASHRAE 2011 Annual Conference*, Montreal, QC, June 25-29, 2011a

Statistics Canada, Energy Supply and Demand Data. (2009). Last visit: February 2014 http://www40.statcan.gc.ca/l01/cst01/prim71-eng.htm

Stephenson, D.G., Mitalas, G.P. (1971) "Calculation of Heat Conduction Transfer Functions For Multi-Layer Slabs" *ASHRAE Transactions*, 77 (Pt2), 117-126

Zmeureanu, R., Fazio, P. (1988) " Thermal performance of a hollow core concrete floor system for passive cooling", *Building and Environment*, 23(3), 243-252